



# THE DEVELOPMENT OF DWDM USING OADM TO INFLUENCE A NON-LINEAR EFFECT SBS

Tomáš Ivaniga<sup>1</sup> and Petr Ivaniga<sup>2</sup>

<sup>1</sup>Department of Electronics and Multimedia Communications, Faculty of Electrical Engineering and Informatics, University of Technology Košice, Košice, Slovakia

<sup>2</sup>Department of Information Networks, Faculty of Management Science and Informatics, University of Žilina, Žilina, Slovakia  
 E-Mail: [tomas.ivaniga@tuke.sk](mailto:tomas.ivaniga@tuke.sk)

## ABSTRACT

In 21<sup>st</sup> century it is not possible to create optical communication lines without software tools simulating a real network under the given conditions. The aim of the article is the development of a DWDM (Dense Wavelength Division Multiplex) system according to the recommendation ITU-T G.694.1. An OADM (Optical add/drop Multiplex) will be incorporated into this system to add or drop particular wavelengths. In total three simulations were planned. The first simulation showed the non-linear effect FWM (Four Wave Mixing) caused by the gaps between the individual channels (50GHz, 25GHz). The second simulation was run in order to increase the bit speed while showing the decrease of BER (Bit Error Rate). The last one was created to illustrate the non-linear effect SBS (Stimulated Brillouin Scattering) in DWDM. The gain changed ( $3 \cdot 10^{-11}$ ,  $2 \cdot 10^{-9}$ ) and two special optical channels were dropped (8 and 15). The whole article is aimed at the decreasing BER and subsequently the related Q-factor in fully optical communications networks.

**Keywords:** BER, DWDM, OADM, SBS.

## 1. INTRODUCTION

In recent years the requirements placed on transfer speed has risen dramatically. People demand more and their goal is to transfer the most amount of data in the shortest possible time. This situation was solved by using optical fibres as the transfer medium offering a great band width and high transfer speed [1], [2]. The optical fibres found their way into telecommunications also due to advantages such as their resistance against electromagnetic influences, ability to transfer information on several wavelengths and a long-distance transfer. Even though the band width of the optical fibres is considered as an advantage, the fibre itself cannot use this bandwidth effectively. This shortcoming started to be compensated via the WDM technologies enabling the transfer of more optical signals in one optical fibre utilising various wavelengths. The WDM technologies became very popular and are commonly used also because their implementation into already existing networks is very simple [3], [4]. The already constructed fibres do not require any additional modification except for the innovation of the transfer systems.

From the currently known WDM technologies the most used are DWDM and CWDM (Coarse Wavelength Division Multiplex) technologies.

## 2. WAVELENGTH-DIVISION MULTIPLEX SYSTEM

Wavelength multiplex is based on the cumulation of several optical channels (previously they were transferred each by a different fibre) into one optical fibre based on the wave multiplex. This technology is closest analogy to the technology of so-called frequency multiplex (FDM - Frequency Division Multiplexing) where the individual transfers are on different frequencies. For WDM the transfers are done by light of various wavelengths. The WDM transfers run through the

transmitter with the multiplexor which connects several signals together. After the travelling through the optical line it goes through the receiver with the demultiplexor and is divided back into the original signals. The concept of such a transfer dates back to late 1970s (this transfer was successfully performed under laboratory conditions in 1978) [2], [5]. Although the functioning principle of WDM is basically simple, the optical devices enabling high transfer capacity are more complicated. They deal with problems as the signal attenuation, noise, chromatic dispersion, polarisation dispersion, mutual interference between neighbouring channels, non-linear effects in the optical fibre and others. The higher demand on the transfer speed, the greater increase in demand on the quality of the active and passive parts. WDM became well known also for enabling increase of the network's capacity without the necessity of additional construction of optical fibres which are newer and of better quality.

The recommendation ITU-T sets 81 channels in band C (195.1 - 191.1THz) with constant gaps of 50GHz on the central frequency 193.1THz. This range can be broadened to L-band (191.4 - 185.9THz) [6]. This band adds another 111 channels with 50GHz gapping. The core parameter of WDM system is its general transfer capacity  $C_{WDM}$  which can be calculated by the following:

$$C_{WDM} = \sum_{k=1}^n v_{pk} \quad (1)$$

where  $v_{pk}$  is the transfer speed of  $k$  channel and  $n$  is the total number of channels of the WDM system. Each channel is given a certain spectral width regardless of it being used or not. When the channel gaps are excessively big, the system attains worse overall spectral effectivity which is defined by



$$\eta_{WDM} = \frac{C_{WDM}}{B_{WDM}}, [\text{bit} \cdot \text{s}^{-1} \cdot \text{Hz}^{-1}] \quad (2)$$

where  $B_{WDM}$  is the total band width taken by WDM system.

### A. Dense wavelength division multiplex

Currently DWDM represents the most advanced variant of WDM. Thanks to DWDM we are able to increase the affectivity of the existing optical fibres multiple times. This of course results in the increase of the transfer fibre capacity [6]. The development of DWDM consisted mostly of the development of components of WDM, foremost the development of the light sources and also the detectors and the optical amplifiers of the EDFA type.

DWDM is characterised by smaller gaps. ITU-T created the standard for DWDMs G.694.1 – Spectral grids for WDM applications: DWDM frequency grid. The standard defines gapping values between individual channels (wavelengths) and they are 0.8nm (100GHz), 0.4nm (50GHz), 0.2nm (25GHz) and 0.1nm (12.5GHz). The standard sets the transfer channels in the range of wavelengths from 1490nm to 1620nm, that is in bands S, C and L[7], [8]. The capacity of one channel is 10Gbps or up to 40Gbps. The number of channels for DWDM ranges from 32 to 160. DWDM uses either 40 transfer channels of gaps of 100GHz, or 80 channels with gaps of 50GHz. The individual transfer channels in THz are counted with gaps of 12.5GHz by the following calculation

$$193.1 + n \cdot 0.0125, \quad (3)$$

where  $n$  can be any integer number of positive or negative sign including zero. With the gap of 25GHz the value 0.0125 changes into 0.025, for the gap of 50GHz it will be the value 0.05 and with the gap of 100GHz the value is 0.1.

The flexible DWDM system is when it is not necessary for every channel gap to be the same. The advantage of the flexible DWDM is that the transfer speed of the channels can vary or even that every channel can use different modulation form. The recommendation ITU-T G.694.1 also defines the flexible DWDM as the width of the individual transfer channels and their nominal medium frequency. The individual nominal medium frequency can be obtained by

$$193.1 + n \cdot 0.00625, \quad (4)$$

where  $n$  can be any integer number less or greater than zero, including zero, and value 0.0625 is nominal medium frequency of granularity in THz [7], [14]. The width of individual channels is defined as 12.5· $m$  where  $m$  is a positive integer number and the value 12.5 is granularity of transfer channel width in GHz.

Any combination of transfer channels is allowed as long as they do not overlap. The example of using

flexible DWDM is shown on Figure-1 where are two transfer channels with the width of 50GHz and two with 75GHz.

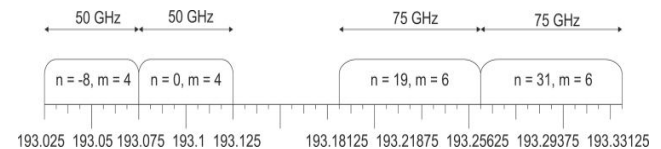


Figure-1. Example of flexible DWDM.

Commercial DWDM systems usually use up to 80 transfer channels with capacity up to 40Gbps which represents the transfer capacity of the fibre up to 3.2Tbps. Also these systems are able to overcome the distance of over 2000km without signal renewal. Current experiments enable transferring several times more intensified data flow but only for the distance of a few hundreds of kilometres [6], [9]. A theoretical presumption is that it will be possible to use up to 1000 transfer channels. The latest discovery was a demonstration of a DWDM with 200 transfer channels capacity of 40Gbps per channel, which produced the total capacity of 8Tbps per fibre.

Technology of DWDM enables every transfer channel to transfer various types of services, such as SONET/SDH, ATM, IP, ATM and similar which contributes to practical systems designed to transfer several types of services.

### B. Coarse wavelength division multiplex

The reason of introduction of CWDM technology was its cost effectiveness. As the CWDM system has greater gaps between individual transfer channels, it results in decreased demand on individual components of the transfer system and thus it is also cheaper. In CWDM systems it is possible to use uncooled laser.

ITU-T issued the recommendation *ITU-T G.694.2 - Spectral grids for WDM applications: CWDM wavelength grid* for CWDM, which defines transfer bands in range of 1270nm to 1610nm [7], [15]. The recommendation defines gaps between individual transfer channels with the value of 20nm.

### 3. OPTICAL ADD/DROP MULTIPLEX

OADM (Figure-2) is a device that selectively drops one wavelength  $\lambda_i$  from a great number of wavelengths  $\lambda_1, \lambda_2, \dots, \lambda_i, \dots, \lambda_N$  multiplexed at their entry to the fibre. It skips (circumvents) all other wavelengths and adds one identical wavelength to the transfer fibre, generally with a different data content [10], [11] and [12]. A general definition of OADM is as a component which:

- demultiplexes some wavelengths entering the fibre and drops them with or without optoelectronic conversion,
- it omits other wavelengths entering from the input fibre to the output fibre,
- it adds wavelengths from local participants to the output fibre by wave multiplexor or joiner,



- it ensures the demultiplexing and multiplexing of the omitted wavelengths with the dropped and added wavelengths.

OADM is either with a dynamically selectable wavelength of with a fixed wavelength. Of course, the most general OXC (Optical Cross-Connector) includes similar options and many technologies enabling OADM and OXC are equal. These technologies use dielectric layered coverage, AWG devices, waveguides connected by grating, MZ (Mach-Zehnder), FP (Fabry-Perot) and other interferometric devices.

The first OADM prototypes were designed around 1980 but the first commercially used OADM networks have emerged only a couple of years ago [13]. Until 2000 they were used mostly in the underground inter-switchboards and underwater networks. However, now they are becoming more and more popular to use in the land access networks. They are often used to circumvent local switchboards. The basic configuration can be divided into three types.

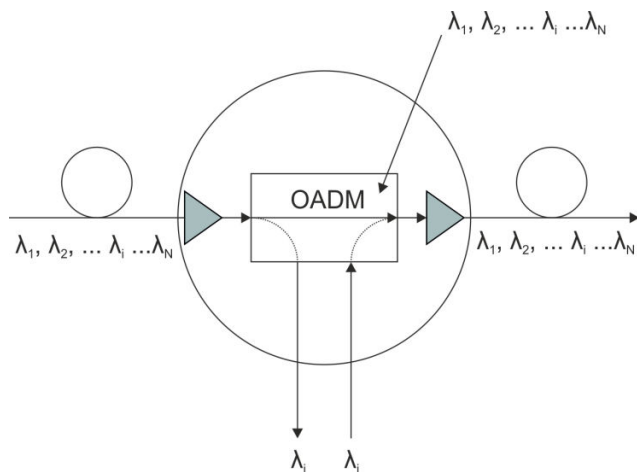


Figure-2. Principle of OADM.

#### A. Configuration add/drop consisting of a grating and two 3dB couplers

At Figure-3 can be observed a simple add/drop configuration consisting of 3dB couplers and a grating in one of the output branches/arms. The light is routed to port 1 and is divided into two parts,  $\lambda_G$  is reflected from the grating and is dropped to port 4. The second coupler of the output port is submerged to the index of corresponding liquid which does not reflect the light. The chosen signal is seen on the input and also the dropped port. The optical isolator on port 1 protects the networks signal input from the retroactively reflected signal. The dropped signal is weaker by 6dB than the original input signal. The second 3dB coupler divides the transferred signal without its reflection from the grating. The add function occurs by routing the signal to port 3 where it is reflected from the grating and is added to signal from port 2, as is shown at Figure-3.

It is necessary to isolate the added port from the signal transmitted from the input by an isolator [16], [31].

When using two isolators (at the input and the specific port) this non-interferometric configuration gives excellent add/drop performance.

In this configuration there are no limits for the length or placement. The ideal grating filters can be designed using the method of inversion scattering [17], [26]. The primary disadvantage of this configuration is the added attenuation for all the channels which is at least 6dB.

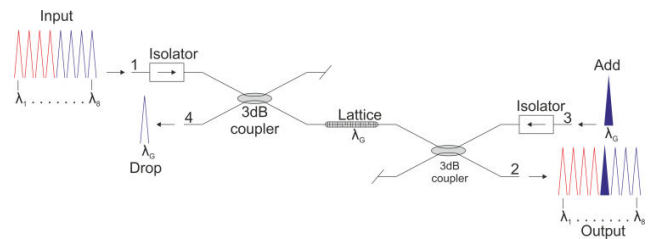


Figure-3. Configuration of the add/drop multiplexor consisting of the grating and two 3dB couplers.

#### B. Configuration add/drop based on interferometry

One of the methods for overcoming a high added loss of the above-mentioned configuration is adding another grating, identical with the first one which created the MZ interferometer [17], [26]. In theory is this device symmetrical and has the potential of performing well considering the added attenuation, backlash reflection and crosstalk.

The principle of this configuration's activity can be observed at Figure-4.

The 3 dB coupler divides the light routed for port 1 and the specific wavelength  $\lambda_G$  is reflected from the second identical grating. These reflected signals meet in the 3dB coupler so the signal is dropped and the back reflection of the light's intensity routing to port equals zero (under the condition that the splitter is well adjusted (50:50 splitter)).

The transmitted wavelengths meet at the second 3dB coupler and enter the output port without residual light from the add port (again, with the well-adjusted coupler) [19], [20]. This configuration is based on the division and interference of light and so is very sensitive on any changes in the length of the signal route, identical grating characteristic and the adjustment of the 3dB couplers.

Several factors are necessary for correct performance of the device: stabilisation of the environment, UV trimming of individual routes, identical couplers and gratings. This configuration has shorter length in the planar technology and is simpler to stabilise. The same gratings can be defined by one exposition simply by a small partition between the arms of the interferometer.

Alternative configurations are based on double-core fibres which act as shorter interferometric arms. They do not need UV trimming [21], [32]. The research showed them as practical devices with configuration based on the MZ interferometers.

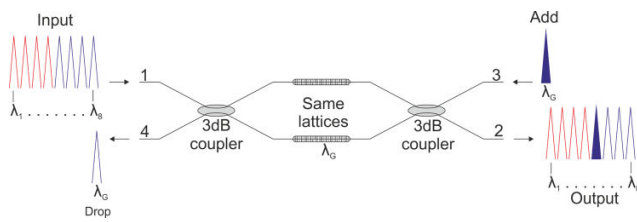


**Figure-4.** Configuration add/drop based on MZ interferometry.

### C. Configuration add/drop consisting of a grating added to the coupler

A stable interferometric add/drop is portrayed at Figure-5. This configuration can be improved by the interference between its own modes of the fibre's coupler.

Recording of the grating in the narrowed part of the half-cycle (100%) of the coupler was evident in both configurations (planar and fibre one) as means of achieving add/drop performance. The device is compact but generally has only the ideal symmetric performance when the grating serves as a purposeless reflector [18], [21], [26]. This is possible only by using very short and firm gratings or very long couplers. This configuration scheme is at Figure-5.

The light is routed to port 1 and is led to even and odd modes of the coupler. The grating is placed in the middle of the coupler where the phase difference between the modes is  $\pi/4$ , i.e. where the light is divided equally between two connected waveguides.

The channel on the resonance wavelength  $\lambda_G$  is reflected from the grating and the remaining signal and the remaining signals go further through the coupler to the output port. At reflection the modes attain the beginning of the coupler with the total phase difference  $\pi/2$ , and the channel is dropped to port 4.

As a general principle, stabilisation of this interferometric device is improved considering the configuration based on MZ interferometers. But the limitation in the grating strength and the length of manufactured couplers can impact expected results.

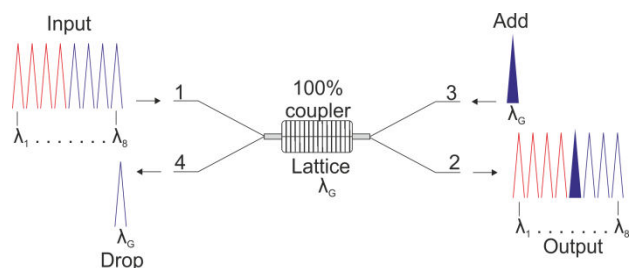


**Figure-5.** Configuration add/drop consisting of grating added to the coupler.

## 4. STIMULATED BRILLOUIN SCATTERING

SBS is a non-linear process occurring in optical fibres with threshold value much lower than in SRS (Stimulated Raman Scattering). Exceeding the threshold value results in generation of the counter Stokes wave which is responsible for most of the input power. Because

of that SBS limits the channel's power in optical communication systems. But it is also possible to practically utilise this effect for the production of optical Brillouin amplifiers and Brillouin lasers.

### A. Basic terminology for SBS and SRS

The non-linear effect SBS was first noticed in 1964 and subsequently studied. SBS is manifested by generating *Stokes* waves whose frequency is shifted towards from the incoming light - by the value dependent from the non-linear medium.

Non-linear effect SBS is similar to the effect SRS but there are some differences between them. The first one is that the Stokes wave in SRS goes in both directions and in the case of SBS only in the backward direction in the case of single-mode fibres. The Stokes shift (approx. 10GHz) is three times smaller for SBS as compared with SRS (approx. 13THz). The threshold value of the pump's power for SBS depends on the spectral width concerning the pump's wave. This value can be as low as 1.1mW for the CW pump, or the pump can be in the form of relatively wide impulses (width  $> 1\mu s$ ). Contrastingly, SBS almost does not occur in the case of short impulses of the pump (width  $< 1ns$ ). For the comparison, the threshold value of power for SRS is approximately 0.5W [22], [23] and [24]. On the other side, the coefficient of Brillouin gain is 100-times greater than at the Raman amplification making SBS a dominant non-linear effect in silicate fibres under some conditions.

It is particularly true for the optical systems using lasers with a narrow linewidth. All these differences spring from one main reason: the acoustic phonons participate in SBS and the optical phonons occur in the case of SRS.

### B. Basic physical principle to describe SBS

The SBS process can be described as a non-linear interaction between the pump Stokes pole and an acoustic wave. The acoustic wave is generated by the process of electrostriction. Electrostriction is the effect inverse to the piezoelectric effect - it is the change of volume or the shape of non-conductors due to the influence from the outer electrical field. The pumping wave creates a pressure wave in the medium through electrostriction. The material density ensures the wave travels the speed of light in the medium in the direction of the pumping wave, creating an acoustic wave. Subsequently, the acoustic wave produces dense modulation resulting in the modulation of the refractory index of the medium. Periodic changes of material density of the fibre seem as a mobile refractory index of the grating. The pump stimulates the index grating causing the scattering of pump light by the Bragg diffraction. A considerable part of the optical power of the pump wave can be converted to the Stokes wave which travels in the opposite direction. Refracted light frequency is also been shifted downwards due to the Doppler shift connected with grating shift of the acoustic speed  $v_A$ . This process is schematically portrayed at Figure-6.

The reaction of material to the pump interference and the Stokes field leads to the increase in the amplitude of the acoustic wave. On the other hand, the impulse



(beating) of pump wave with the acoustic wave has the tendency to strengthen the Stokes wave. This explains the outlook of the SRS process. The same process of refraction can be observed in quantum mechanics as the expiration of pump photons which create both the Stokes waves and the acoustic photons at the same time. As both energies and dynamics must be preserved during each refraction so the frequencies and the wave vectors of the three waves are inter-dependent by these:

$$\Omega_B = \omega_p - \omega_s, \tag{5}$$

$$k_A = k_p - k_s, \tag{6}$$

where  $\omega_p$  and  $\omega_s$  are frequencies, and  $k_p$  and  $k_s$  are vectors of the pump waves and Stokes waves.

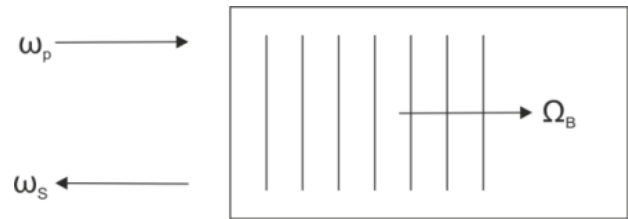


Figure-6. Schematic illustration of the SRS process.

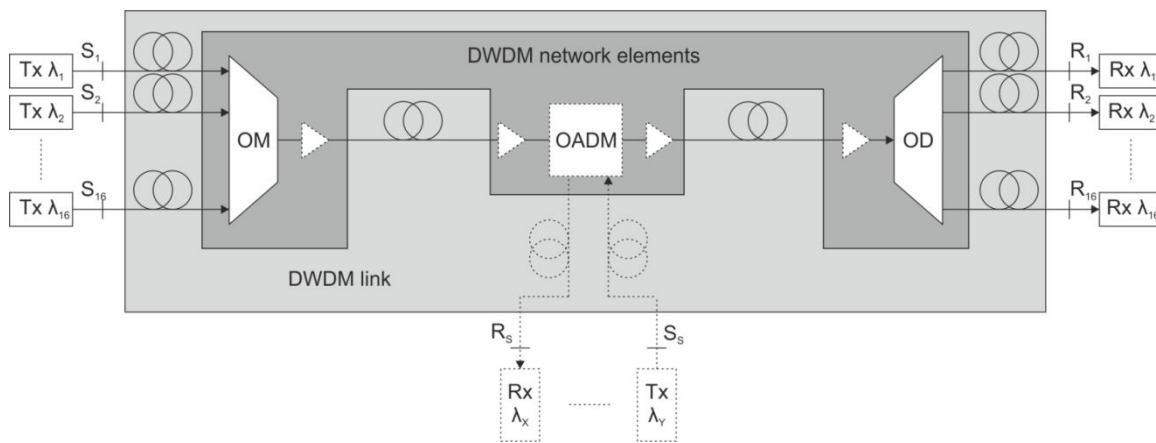


Figure-7. Design of DWDM using OADM.

Frequency  $\Omega_B$  and vector of wave  $k_A$  from the acoustic wave meet the standard of the dispersion calculation

$$\Omega_B = v_A |k_A| \approx 2v_A |k_p| \sin(\theta/2), \tag{7}$$

where  $\theta$  is the angle between the pump and the Stokes pole - from the equation (6) it was presumed that  $|k_p| \approx |k_s|$ . The equation (7) expresses the frequency shift by the Stokes wave dependent on the angle of scattering [25], [26]. Mainly in the case when  $\Omega_B$  is maximal and in the opposite direction ( $\theta = \pi$ ) and with zero (negligible) value in the direct direction ( $\theta = 0$ ). For the single-mode fibre the only important directions are the direct one and the reverse one. For this reason SBS still remains only in the reverse direction with the Brillouin shift with the value of

$$v_B = \Omega_B / 2\pi = 2n_p v_A / \lambda_p, \tag{8}$$

where from the calculation (7) were used  $|k_p| = 2\pi n_p / \lambda_p$ , where  $\lambda_p$  is the wavelength of the pump wave and  $n$  is the refractory index of the fibre. When we use values  $v_A = 5.96 \text{ km/s}$  and  $n_p = 1.45$ , which are typical values for the silicate fibre, the Brillouin frequency shift is achieved  $v_B = 11.5 \text{ GHz}$  while  $\lambda_p = 1550 \text{ nm}$  [27], [28]. Despite the equation (7) assumes correctly that SBS should happen

only in the reverse direction in the single-mode fibres (SMFs) but SBS can occur also in the direct direction [29], [30]. A small amount of Stokes light is generated in the direct direction. This effect is termed as the "controlled acoustic wave" of the Brillouin scattering.

In practice it expresses the Stokes spectrum with several lines with a shifted frequency in the range from 10 to 1000 MHz.

### 5. CONSTRUCTION OF DWDM USING OADM TO VERIFY THE SBS EFFECT

The aim of the optical communication system was to achieve a many-channel transfer for the distance of the metropolitan network (which exceeds to the distance of 120 km). The request on the multiplexing technology was placed on the modern WDM technology with the option to use the recommendation ITU-T G.694.1 (DWDM). The other request was to use OADM in the design of the optical communication system. According to the stated requirements the optical communication was designed - with its simplified scheme at Figure-7. A 16-channel system was chosen for the construction, i.e. 16 transmitters and 16 receivers. The gaps between the transfer channels varied (50 GHz and 25 GHz) which is standard for DWDM. Transfer speed per one transfer channel was 10 Gbps meaning the total transfer speed in the optical fibre reached up to 160 Gbps. The designed OADM belongs among the fixed OADM because the



simulation programme does not allow setting particular parameters for the reconfigurable OADM (ROADM).

Our OADM has the option to add/drop two transfer channels. The overall transfer distance is 120km and is divided into two parts where is placed the already mentioned OADM. Transfer distances are homogeneously divided into 60km sections.

Signals from individual transmitters are joined into the optical fibre by an optical multiplex. The optical multiplex enables the placement of several wavelengths into one shared fibre enabling the capacity multiplication of the fibre. This component can be set with the same attenuation on each input (the symmetric multiplex) or with a different attenuation for each input (non-symmetrical multiplex). When the attenuation is set to 0dB, the component represents the ideal multiplex without the attenuation - it adds the input signals perfectly. For the

simulation purposes the ideal multiplex was utilised. On the line are optical amplifiers with the input power of 8dBm.

The noise figure NF of the amplifiers can be defined by the data file of the scalar number.

In our case NF is defined by the scalar number and its value is 5.5dB. The signal is then routed to the optical fibre and transferred to the optical splitter. It used the single-mode fibre with the attenuation  $0.25\text{dB}\cdot\text{km}^{-1}$ . The received signal is divided into the individual receivers with the help of optical demultiplex. The OADM is placed into the line with the task of adding and dropping specific channels without the need for the multiplexed signal to transfer from the optical to the electrical region. In our case, through OADM were dropped two channels and consequently on those exact frequencies another channels were added (Section V. D).

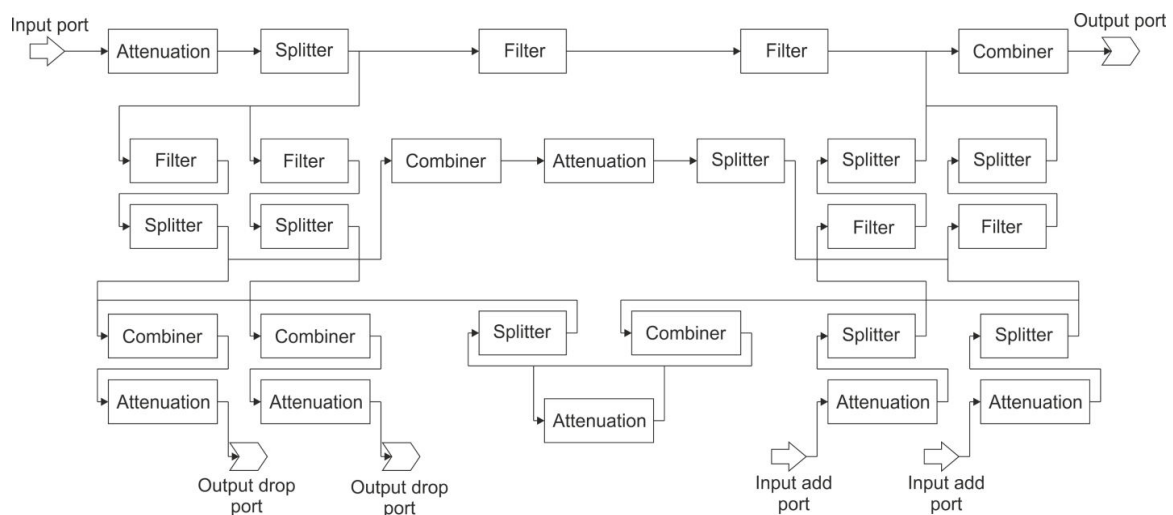


Figure-8. Construction of OADM.

## A. Design of the transmitter, receiver and the construction of OADM

### a) Transmitting part

Basic blocks are: data source, laser, modulator, coding. The data source has the task of generating the random sequence of bits. The data source is connected to the NRZ block through the logical port. Transfer speed is set by the data source, which is 10Gbps. The NRZ block provides link coding - it is possible to set the size of the transmitting levels of the individual states. The resistibility of the transfer channel can be influenced by changing the sizing of the transmitting levels. Naturally, the resistibility of the transfer channel increases with greater differences between the transmitting levels and, on the contrary, decreases it with a smaller difference. In our case the transmitting levels were set to 2.5V (for logic „1“) and -2.5V (logic „0“). In CW laser block power, its spectral height and the transmitting frequency are set. The transmitting power of CW laser is set to 0.1mW. The spectral height marked as FWHM (Full Width at Half Maximum) is set to 10MHz.

The last block of transmitter is optic modulator consisting of two input ports and one output port. One input port is electric connected through to the NRZ block. The second input port is optical and is connected through to the output port of CW laser. The output port is optical. The function of the optical modulator is to modulate the optical signal coming from the CW laser based on the electric signal and the electric signal is being modulated by the link code of NRZ. From the block of the optical modulator the optical signal goes to the output port of the transmitter itself (the input port of the multiplex).

### b) Receiving part

The second modulated block consists of these components: optical filter, PIN and electrical filter. The receiver has the function to convert the optical signal to the electrical. Our modulated receiver detects one particular transfer channel and this is ensured by the optical filter. The optical band pass filter is of the width 20MHz (decrease by 3dB). From the optical filter the optical signal goes to PIN photodiode converting the optical signal to electric one. The quantum efficiency of PIN was set to 81%. Consequently the electric signal goes



through the electric filter and to the receiver's output. The receiver's output is connected to the measuring block where it is possible to record the error rate of the individual channels (BER and related Q-factor).

### c) OADM

The last modulated block is OADM. This block consists of these components: attenuation block, optical band stop filter, optical band pass filter, optical splitter, optical combiner (Figure-8).

The attenuation block at the input represents the input attenuation of OADM. Value of the attenuation block was set to 3dB. Designed OADM consists of two branches and it branches out after the attenuation block. This branching occurs in the optical splitter following the attenuation block. In the first branch (upside) there are two optical band stop filters connected one after the other with the task of blocking the frequencies of the transfer channels that are added/dropped.

The second (downside) branch can be divided into two parts, the adding and the dropping one. The dropping one has been assigned the task of dividing the specific channels from all the other transfer channels. This is done by the splitter branching the OADM and the optical band pass filter filtering only particular channels. The filtered optical signal then proceeds through the optical splitter and the combiner. Then the optical signal goes to the output port of OADM via the attenuation block representing the attenuation of the dropped channels. The adding part of OADM is very similar to the dropping part except for the change of direction.

So the attenuation block represents the input attenuation of the added channels. After the attenuation block are placed the optical splitter and the combiner and at last the band pass filter. This filter has the same parameters as the one in the dropping part of the optical filter. All filters are of the identical band width whether it is the band pass or band stop type for the reason not to cause cross-talk at the joining of the upside and the downside branches.

It is the mentioned optical splitters and combiners in both parts of the downside branch that are modelling the cross-talk between the channels of the dropped and added parts. Both modelled cross-talks are identical with the exception of the direction. The upside branch cross-talk influences the added channels from the dropped ones and contrary to that, the downside branch influences the dropped channels based on the added channels. The attenuation blocks in the cross-talk branches specify the value of cross-talk.

Values of these attenuation blocks does not need to equal meaning that it is possible to set greater values of cross-talk for one direction than the other. The values in our case are identical, which is 30dB each. The whole design of OADM in the programme *OptSim* is shown at Figure-8.

### B. Simulation at the change of gaps between the channels

The aim of the simulation was to show the non-linear effect FWM connected with the channel gaps. This effect is demonstrated by the increase of BER and a decrease in Q-factor. At Figure-9a can be observed the eye diagram with the gaps of 50GHz and at Figure-9b is the eye diagram with the gaps of 25GHz.

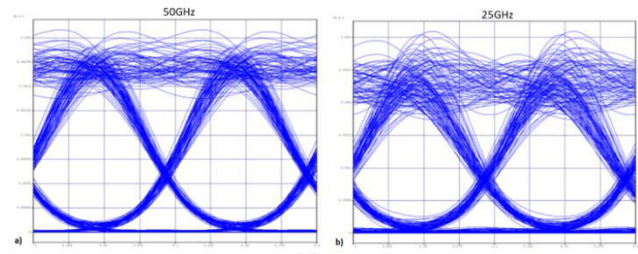


Figure-9. Eye diagram with the gaps of 50GHz and 25GHz.

With the channel gaps of 50GHz error rate was  $BER=1.42 \cdot 10^{-18}$  and with channel gaps of 25GHz it was  $BER=4.75 \cdot 10^{-12}$ . The channel gapping has a great influence on BER - as the gap decreases, it causes interference resulting in wrong evaluation of the symbol.

### C. Simulation of the change of transfer speed

The aim of this simulation was the comparison of BER at bit speed  $10\text{Gbit.s}^{-1}$  (Figure 10a) and  $20\text{Gbit.s}^{-1}$  (Figure 10b). It is obvious that with the increasing bit speed BER will decrease. With the transfer speed of 10Gbps Q-factor is 10.41dB and error rate is  $1.34 \cdot 10^{-18}$ , which is a negligible value. When the transfer speed is increased to 20Gbps error rate reaches 0.02275, Q-factor falls to 2.02 and the eye diagram is completely unclear. This means that the system is considered as acceptable when BER does not exceed  $10^{-11}$ .

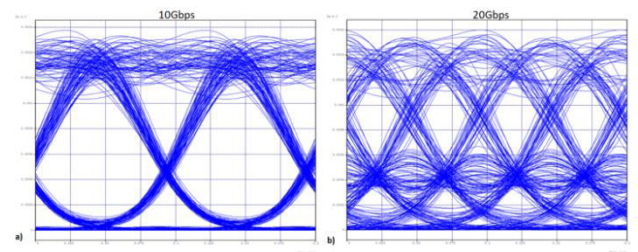


Figure-10. Eye diagram at bit speed 10Gbps and 20Gbps.

### D. Simulation for observing the SBS effect

The aim of this simulation was the change of gain in OADM. Figure-11 shows 2 spectra with various values of SBS. The red curve represents the output spectrum with the gain value of  $3 \cdot 10^{-11}$  and the blue curve represents the spectrum of the output with  $2 \cdot 10^{-9}$ . With the transmitting and amplifying power the threshold value exceeded at SBS gain of  $2 \cdot 10^{-9}$ .

Because these spectra were from the ends of the system after the amplification, the intensifying of the



threshold value was manifested by the increase of the side noise (Figure-11), approximately about 10dB. It is caused by the scattering of the useful signal in fibre and thus it decreases its value at the output - and although it gains back its original value after amplification it is with the side noise.

At Figure-12 is the spectrum before the optical amplifier with the value of SBS gain  $3 \cdot 10^{-11}$  (green curve) and  $2 \cdot 10^{-9}$  (red curve). Also noteworthy at Figure-12 is the peak value of SBS gain  $2 \cdot 10^{-9}$  is lower by approximately 10dB than the peak value of SBS gain  $3 \cdot 10^{-11}$ . At the end it always means the worsening of the SNR value which naturally has its influence on BER.

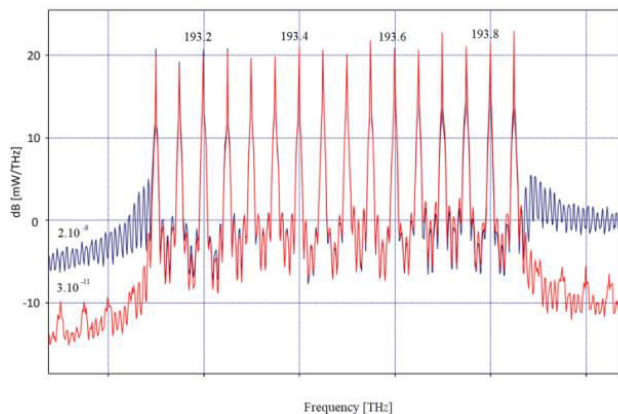


**Figure-11.** Spectra comparison at the end of DWDM with SBS gain values of  $3 \cdot 10^{-11}$  (red curve) and  $2 \cdot 10^{-9}$  (blue curve).

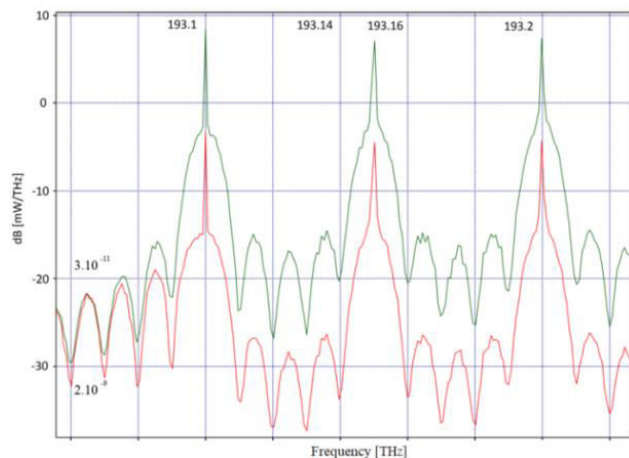


**Figure-12.** Spectra comparison at the end of the first fibre before the optical amplifier. The green curve is SBS gain  $3 \cdot 10^{-11}$  and the red curve is gain  $2 \cdot 10^{-9}$ .

At Figure-11 or at Figure-12 the SBS wave is not visible because the spectra were taken from the ends of the fibre and the SBS wave flows in the backward direction. The SBS wave could be found at the beginning of the optical fibre but the problem was that the simulation programme did not logically allow the inter-connection of two block inputs (fibre's input and the entryway of the measuring block).

In Table-1 is the comparison of BER with the SBS gain of  $3 \cdot 10^{-11}$  and  $2 \cdot 10^{-9}$  for the transfer channels 5, 8, 13 and 15. The transfer channels 8 and 15 were monitored not at the ends of the communication system but at the outputs of OADM (referred to as „drop 8“ and „drop 15“).

In comparison of these two channels and the channels 5 and 13 can be observed the SBS effect does not influence linearly. The BER worsening in channels 8 and 15 (with shorter distance) happened by about 9 grades and in channels 5 and 13 generally only by about 6 grades. In case of the designed scheme the fibre used would have had the SBS gain under the value of  $2 \cdot 10^{-10}$  to attain acceptable BER.

**Table-1.** BER for different channels.

Number of transfer channel	BER at SBS gain $3 \cdot 10^{-11}$	BER at SBS gain $2 \cdot 10^{-9}$
5	$1.006 \cdot 10^{-12}$	$1.323 \cdot 10^{-6}$
13	$4.475 \cdot 10^{-14}$	$3.407 \cdot 10^{-7}$
drop 8	$2.514 \cdot 10^{-24}$	$4.494 \cdot 10^{-15}$
drop 15	$4.882 \cdot 10^{-34}$	$4.362 \cdot 10^{-23}$

## 6. CONCLUSIONS

The main aim of the article was to design a full optical communication system with BER not falling beneath the value of  $10^{-11}$ . DWDM system was designed with the gaps of 50GHz and bit speed of 10Gbps so the values of Q-factor would be acceptable for the output of each one channel. The construction proceeded with coding of NRZ type because in past these link codes were used: Manchester, Miller, BRZ which did not attain such good values when compared with NRZ. The construction of OADM was created in the programme OptiSim (Figure-8).

For OADM were chosen particular wavelengths showing that with SBS gain  $3 \cdot 10^{-11}$  it is possible to reach better values as with SBS gain  $2 \cdot 10^{-9}$ . At Figure-11 and Figure-12 are the individual spectra influenced by SBS gain.

## ACKNOWLEDGEMENT

This work was supported by research grant KEGA no. "023TUKE-4/2017".

## REFERENCES

- [1] Papan J., Drozdova M., Segec P., Mikus L., Hrabovsky J. 2015. The new PIM-SM IPFRR mechanism. ICETA 2015 - 13th IEEE International Conference on Emerging eLearning Technologies and Applications, Proceedings, art. no. 7558504, 1-7, doi: 10.1109/ICETA.2015.7558504.
- [2] Ivaniga P., Ivaniga T. 2017. 10 Gbps optical line using EDFA for long distance lines. Przegląd Elektrotechniczny. 93(3):193-196.



- [3] Smiesko J., Uramova J. 2012. Access node dimensioning for IPTV traffic using effective bandwidth. *Komunikacie*. 14(12):11-16.
- [4] Pavlik M., Kruželák L., Mikita M., Špes M., Bucko S., Lisoň L., Kosteres M., Beňa E., Liptai P. 2017. The impact of electromagnetic radiation on the degradation of magnetic ferrofluids, *Archives of Electrical Engineering*. 66(2):361-369.
- [5] Steingartner W., Novitzká V. 2016. Categorical model of structural operational semantics for imperative language. *Journal of Information and Organizational Sciences*. 40(2):203-219.
- [6] Tóth J., Ovseník L., Turán J. 2015. An overview of various types of waveguide grating based demultiplexors in WDM systems. In: *IWSSIP 2015*. - London : City University. pp. 29-32.
- [7] Hamza M. Y., Hayee I. 2016. Performance improvement of 40 Gb/s WDM systems by optimization of dispersion map. 2016 IEEE 10<sup>th</sup> International Conference on Application of Information and Communication Technologies (AICT), 1-5. doi: 10.1109/ICAICT.2016.7991755.
- [8] Ivaniga T., Ivaniga P. 2017. Comparison of the Optical Amplifiers EDFA and SOA Based on the BER and Q-Factor in C Band. *Advances in Optical Technologies*, vol. 2017, ID 9053582, 9. doi:10.1155/2017/9053582.
- [9] Skorpil V., Precechtel R. 2013. Training a neural network for a new node element design. *Przegląd Elektrotechniczny*. 89(2B):187-192.
- [10] Ivaniga P., Ivaniga T. 2017. Comparison of DPSK and RZ-DPSK Modulations in Optical Channel with Speed of 10 Gbps. *Journal of Information and Organizational Sciences*. 41(2):185-196.
- [11] Vardanyan V. 2016. Single-fiber optical transmission system with DWDM channels effect of four-wave mixing products, 2016 13<sup>th</sup> International Scientific-Technical Conference on Actual Problems of Electronics Instrument Engineering (APEIE), 23-25. doi: 10.1109/APEIE.2016.7806431.
- [12] Steingartner W., Novitzká V. 2015. A new approach to semantics of procedures in categorical terms. 2015 IEEE 13<sup>th</sup> International Scientific Conference on Informatics, Poprad. 252-257.
- [13] Mikúš L. 2003. Available tools for the educational course development. *ICETA 2003: 2nd international conference on emerging telecommunications technologies and applications and the 4th conference on virtual universit, Košice: Technical University*. pp. 295-297.
- [14] Figuli L., Smieško J. 2014. Recognition and modelling of bursty period of flow. *WSEAS Transactions on Communications*. 13:444-451.
- [15] Abdullaev A., Turán J. 2014. Survey of the problems and solutions of arrayed waveguide gratings used in the optical networks. *Acta Electrotechnica et Informatica*. 14(3):49-53. doi: 10.15546/aei-2014-0029.
- [16] Sifta R., Munster P., Krajsa O., Filka M. 2014. Simulation of bidirectional traffic in WDM-PON networks. *Przegląd Elektrotechniczny*. 90(1):95-100. doi:10.12915/pe.2014.01.23.
- [17] Bachrata K. 2003. Effective bandwidth for deterministic networks. *Komunikacie*. 1(4): 78-82
- [18] Ivaniga P., Ivaniga T., Turán J., Ovseník L., Márton M., Solus D., Oravec J., Huszaník T. 2018. The Influence of FWM with AWG Multiplexor in DWDM System. *Przegląd Elektrotechniczny*. 94(4):113-117. doi:10.15199/48.2018.04.28.
- [19] Mikus L., 2010. Evaluations of the Error Rate in Backbone Networks. *Elektrorevue*. 12(2):1-6.
- [20] Papán J., Segeč P., Drozdová M., Mikuš L., Moravčík M. and Hrabovský J. 2016. The IPFRR mechanism inspired by BIER algorithm. 2016 International Conference on emerging eLearning Technologies and Applications (ICETA), Vysoké Tatry. 257-262. doi: 10.1109/ICETA.2016.7802053.
- [21] Huszaník T., Turán J., Ovseník L. 2018. Comparative Analysis of Optical IQ Modulation in Four-channel DWDM System in the Presence of Fiber Nonlinearities. In: *ICCC 2018 - 19<sup>th</sup> International Carpathian Control Conference*. 468-473.
- [22] Ruzbarsky J., Turan J., Ovseník L. 2015. Effects act on transmitted signal in a fully optical fiber WDM systems. 2015 IEEE 13<sup>th</sup> International Scientific Conference on Informatics. 217-221.
- [23] Bhatia K. S., Kamal T. S. 2013. Modeling and simulative performance analysis of OADM for hybrid



multiplexed Optical-OFDM system. *Optik*. 124:1907-1911.

- [24] Roka R., Mokráň M. 2018. Effect of the FWM influence on the CWDM signal transmission in the optical transmission media. *International Journal of Circuits, Systems and Signal Processing*. 12:42-47.
- [25] Smieško J. 2014. IP Network Management of Source for IP Traffics. *Scientific Papers of the University of Pardubice. Series D, Faculty of Economics & Administration*. 21(32):109-117.
- [26] Abdullaev A., Turan J. 2014. Analysis of the Methods of Preventing of Contention Resolution in Optical Packet Switching Networks. *Carpathian Journal of Electronic and Computer Engineering*, 7(1):3-6.
- [27] Ivaniga T., Ivaniga P., Turán J., Ovseník L. 2017. Analysis of possibilities of increasing the spanned distance using EDFA and DRA in DWDM system. *Komunikácie*. 19(3):88-95.
- [28] Nain H., Jadon U., Mishra V. 2016. Evaluation and analysis of non-linear effect in WDM optical network, 2016 IEEE International Conference on Recent Trends in Electronics, Information & Communication Technology (RTEICT). pp. 36-39.
- [29] Bosternak Z., Roka R. 2018. Bandwidth Scheduling Methods for the Upstream Traffic in Passive Optical networks. *Przeglad Elektrotechniczny*. 94(4):9-12. doi:10.15199/48.2018.04.03.
- [30] Ruzbarsky J., Turan J., Ovsenik L. 2016. Stimulated Brillouin scattering in DWDM all optical communication systems. 2016 26th International Conference Radioelektronika, Kosice. 395-398. doi: 10.1109/RADIOELEK.2016.7477354.
- [31] Liptai P., Dolník B., Pavlík M., Zbojovský J., Špes M. 2017. Check measurements of magnetic flux density: Equipment design and the determination of the confidence interval for EFA 300 measuring devices, *Measurement*. 111:51-59.
- [32] Márton M., Ovseník L., Turán J., Špes M., Vásarhelyi J. 2018. Possibility of increasing availability of FSO/RF hybrid system with implementation of helix antenna for 5.2GHz. In: *ICCC 2018 - 19<sup>th</sup> International Carpathian Control Conference*. 498-501.